

## Keggin Ions as UV-Switchable Reducing Agents in the Synthesis of Au Core–Ag Shell Nanoparticles

Saikat Mandal, PR. Selvakannan, Renu Pasricha, and Murali Sastry\*

Materials Chemistry Division, National Chemical Laboratory, Pune-411 008, India

Received March 4, 2003; E-mail: sastry@ems.ncl.res.in

Bimetallic nanoparticles, either as alloys or as core–shell structures, exhibit unique electronic, optical, and catalytic properties<sup>1–4</sup> and have important biological applications in DNA sequencing.<sup>5</sup> Alloy nanoparticles may be conveniently synthesized by simultaneous reduction of two or more metal ions,<sup>3</sup> while growth of core–shell structures may be accomplished by the successive reduction of one metal ion over the core of another.<sup>4,6</sup> The latter process often leads to the formation of fresh nuclei of the second metal in solution, in addition to a shell around the first metal core,<sup>6</sup> and is clearly undesirable from the application point of view. A possible strategy to overcome this drawback could be based on immobilization of a reducing agent on the surface of the core metal which, when exposed to the second metal ions, would reduce them, thereby leading to the formation of a thin metallic shell (Figure 1A).

Polyoxometalates such as Keggin ions undergo stepwise multi-electron redox processes without structural change<sup>7</sup> and may be reduced electrolytically, photochemically, and with suitable reducing agents. Troupis, Hiskia, and Papaconstantinou have shown that exposure of photochemically reduced [(SiW<sub>12</sub>O<sub>40</sub>)<sup>4-</sup>] Keggin ions to aqueous Ag<sup>+</sup>, Pd<sup>2+</sup>, AuCl<sub>4</sub><sup>-</sup>, and PtCl<sub>6</sub><sup>2-</sup> ions resulted in the formation of stable metal nanoparticles capped by the Keggin ions.<sup>8</sup> It should be possible, in principle, to reduce the surface-bound Keggin ions by further UV irradiation and use them as highly localized reducing agents in the synthesis of metal core–shell nanoparticles, as discussed below for the case of Au core–Ag shell nanostructures.

To 30 mL of 10<sup>-2</sup> M aqueous deaerated solution of phosphotungstic acid [PTA, H<sub>3</sub>(PW<sub>12</sub>O<sub>40</sub>), obtained from Aldrich and used as-received, solution pH 2.5] was added 2 mL of propan-2-ol, and the mixture was irradiated by UV light for 4 h (Pyrex filter, >280 nm, 450-W Hanovia medium-pressure lamp; step 1, Figure 1A). This leads to reduction of (PW<sub>12</sub>O<sub>40</sub>)<sup>3-</sup> ions and is seen as a blue color appearing in the solution (test tube 1, inset of Figure 1B). The UV–vis spectrum of this solution (curve 1, Figure 1B) shows the presence of an absorption band at 760 nm that is characteristic of one-electron-reduced PTA, [PW<sub>12</sub>O<sub>40</sub>]<sup>4-</sup>.<sup>7,9</sup> To 5 mL of this irradiated PTA solution was added 15 mL of 10<sup>-3</sup> M HAuCl<sub>4</sub> solution under continuous stirring for 10 min, and then the solution was allowed to age for 2 h (step 2, Figure 1A). The solution changed color from blue to pink (test tube 2, inset of Figure 1B), indicating formation of gold nanoparticles. The UV–vis spectrum recorded from the PTA–gold solution (curve 2, Figure 1B) shows a fairly sharp absorption band centered at 540 nm due to excitation of surface plasmon vibration in gold nanoparticles.<sup>3a</sup> This solution was extremely stable over time, indicating that the Keggin ions are bound to the nanoparticle surface and stabilize them electrostatically and stereochemically (Figure 1A, step 2).<sup>8,10</sup>

Uncoordinated PTA ions in solution were removed by thoroughly dialyzing the PTA–gold nanoparticle solution against distilled water for 2 days, using a 12K cutoff dialysis bag. The dialyzed solution was also extremely stable over time. The presence of Keggin ions

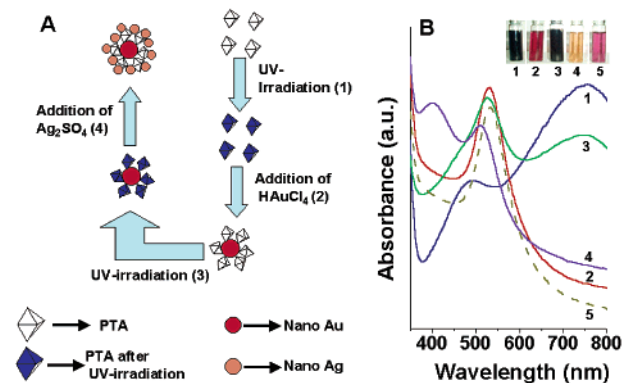


**Figure 1.** (A) Scheme of the Keggin ion-mediated synthesis of Au core–Ag shell nanoparticles. For simplicity, Keggin ions are shown as octahedral particles. (B) UV–vis spectra recorded from (1) 10<sup>-2</sup> M aqueous solution of PTA after UV irradiation; (2) UV-irradiated PTA solution after addition of 10<sup>-3</sup> M HAuCl<sub>4</sub>; (3) solution 2 after further UV irradiation; (4) solution 3 after addition of 10<sup>-3</sup> M Ag<sub>2</sub>SO<sub>4</sub> solution; and (5) solution 2 after addition of 10<sup>-3</sup> M Ag<sub>2</sub>SO<sub>4</sub>. All UV–vis spectra have been adjusted for solution dilution effects. Pictures of sample bottles containing solutions 1–5 are shown in the inset (see text for details).

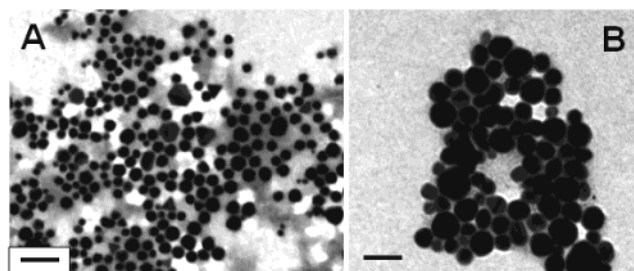


**Figure 2.** (A) TEM picture of gold nanoparticles reduced by UV-irradiated PTA solution. (B) TEM picture of gold core–silver shell nanoparticles by sequential reduction of gold and silver ions by UV-irradiated PTA solution. Scale bars in A and B correspond to 100 and 50 nm, respectively.

in the dialyzed PTA–nanogold solution was established by X-ray diffraction analysis of a drop-cast film on a glass substrate (Supporting Information, Figure S1, curve 2). The Bragg reflections characteristic of fcc gold are identified in this XRD pattern, clearly indicating that the particles are nanocrystalline. Characteristic Bragg reflections from the Keggin ions are observed (Figure S1, curve 1),<sup>11</sup> indicating that UV activation and reduction of AuCl<sub>4</sub><sup>-</sup> ions has not disturbed their basic structure.

Figure 2A shows a representative low-magnification transmission electron microscopy (TEM) image of PTA–gold nanoparticles.<sup>12</sup> The nanoparticles are polydisperse (size ranging from 15 to 70 nm) and of irregular morphology. Figure 3A shows a high-resolution TEM image of one of the gold nanoparticles. The contrast is uniform throughout the particle, thus indicating that it is a single nanocrystal. A number of multiply twinned gold nanoparticles could

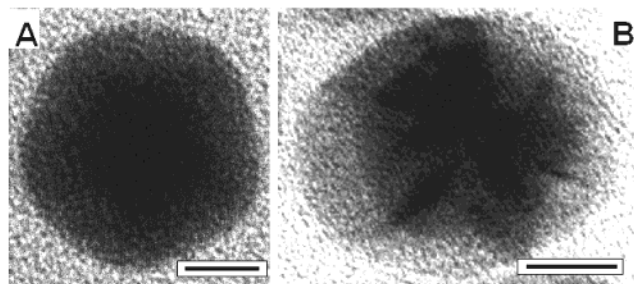


**Figure 3.** (A) High-resolution TEM image of one of the gold particles. (B) High-resolution TEM image of one of the Au core–Ag shell particles. Scale bars in A and B correspond to 5 and 10 nm, respectively.

also be observed, which at higher magnification clearly showed the lattice planes of fcc gold.

Following dialysis of the PTA–gold nanoparticle solution, it was UV-irradiated again for 4 h (step 3, Figure 1A). The UV–vis spectrum of the PTA–gold nanoparticle solution after irradiation is shown as curve 3 in Figure 1B. The solution color changed from pink to a bluish-red (test tube 3, inset of Figure 1B) and was accompanied by an increase in absorption at 760 nm. The increase in absorption at long wavelengths clearly indicates that the PTA ions on the surface of the gold nanoparticles have been reduced. To 15 mL of this solution was added 15 mL of  $10^{-3}$  M aqueous solution of  $\text{Ag}_2\text{SO}_4$  under stirring (step 4, Figure 1A). Within 15 min, the solution changed color to a light brown (test tube 4, inset of Figure 1B). The UV–vis spectrum from this solution (curve 4, Figure 1B) shows a damping and blue shift of the gold surface plasmon vibration band, accompanied by the appearance of a distinct absorption band centered at 415 nm. These observations are symptomatic of formation of silver shells around the PTA-capped gold nuclei, as depicted in the scheme in Figure 1A.

Figure 2B shows a representative TEM picture of a drop-cast film of Au core–Ag shell nanoparticles grown as described above.

As in the case of gold nanoparticles alone, the particles are quite polydisperse, show a small increase in size (ranging from 20 to 100 nm), and are of varying morphology. A high-resolution TEM image of one Au core–Ag shell nanoparticle is shown in Figure 3B. A distinct variation in contrast between the dark gold core and the lighter silver shell is clearly seen. The thickness of the shells varied across particles and often exhibited morphology different from that of the core. Spot-profile energy-dispersive analysis of X-rays (EDX)<sup>12</sup> of a number of large Au core–Ag shell particles yielded an average Au:Ag molar ratio of 3:1 in the core region, while in the shell region the ratio changed to 1:10. This clearly indicates that the shell in Figure 3B corresponds to silver, the small gold signal possibly being due to beam diameter effects in EDX. Spot-profile EDX analysis of a number of particles always revealed the presence of both Au and Ag signals, indicating that nucleation of fresh Ag nanoparticles had not occurred.

A control experiment was performed wherein  $\text{Ag}^+$  ions were added to the PTA-capped gold nanoparticle *without* additional UV

irradiation (test tube 5, inset of Figure 1B). Little change in the solution color occurred (compare test tubes 2 and 5, inset of Figure 1B) and was supported by negligible changes in the solution UV–vis spectra before (curve 2, Figure 1B) and after ion exposure (curve 5, Figure 1B). Curve 5 alone has been marginally shifted down since it was identical to curve 2). Thus, photochemical charging of PTA molecules bound to the gold nanoparticle surface is the crucial step in this work that sets it apart from other bimetallic nanoparticle core–shell synthesis protocols that employ reducing agents present uniformly in the reaction medium. That the reducing capability of the Keggin ions can be switched on using UV irradiation is an additional feature that enhances the versatility of the technique.

In summary, the formation of Au core–Ag shell nanoparticles using photochemically reduced phosphotungstate Keggin ions has been described. The use of Au nanoscale surface-bound switchable reducing agents such as that provided by Keggin ions enables the reduction of  $\text{Ag}^+$  ions only on the surface of the gold particles, thus obviating the possibility of nucleation of fresh Ag nanoparticles in solution. Preliminary studies have shown that it is possible to realize Au core–Pt shell nanostructures using Keggin ions, thus generalizing the new strategy for realizing bimetallic core–shell structures using Keggin ions with potential application in nanomaterials synthesis and catalysis.

**Acknowledgment.** S.M. and P.R.S. acknowledge the University Grants Commission and Council of Scientific and Industrial Research, Government of India, for financial support. We thank Prof. C. N. R. Rao for use of HRTEM facilities at the JNCASR in Bangalore.

**Supporting Information Available:** XRD patterns of films of PTA and PTA-Au nanoparticles showing retention of the Keggin structure and crystalline nature of the gold particles (PDF). This material is available free of charge via the Internet at <http://pubs.acs.org>.

## References

- (1) Schmid, G. *Clusters and Colloids*; VCH: Weinheim, 1994.
- (2) Toshima, N.; Yonezawa *New J. Chem.* **1998**, *11*, 1179.
- (3) (a) Link, S.; Wang, Z. I.; El-Sayed, M. A. *J. Phys. Chem. B* **1999**, *103*, 3529. (b) Mallin, M. P.; Murphy, C. J. *Nano Lett.* **2002**, *2*, 1235.
- (4) Ah, C. S.; Hong, S. D.; Jang, D.-J. *J. Phys. Chem. B* **2001**, *105*, 7871.
- (5) Cao, Y.-W.; Jin, R.; Mirkin, C. A. *J. Am. Chem. Soc.* **2001**, *123*, 7961.
- (6) Srnova-Sloufova, I.; Lednický, F.; Gemperle, A.; Gemperlova, J. *Langmuir* **2000**, *16*, 9928.
- (7) Papaconstantinou, E. *Chem. Soc. Rev.* **1989**, *18*, 1.
- (8) Troupis, A.; Hiskia, A.; Papaconstantinou, E. *Angew. Chem., Int. Ed.* **2002**, *41*, 1911.
- (9) In the pH range 2–6,  $[\text{PW}_{12}\text{O}_{40}]^{3-}$  ions are known to convert reversibly to  $[\text{PW}_{11}\text{O}_{39}]^{7-}$  ions [Pope, M. T. *Heteropoly and Isopoly Oxometalates*; Inorganic Chemistry Concepts 8; Springer-Verlag: New York, 1983; Chapter 4]. Such hydrolyzed ions may also be active in gold ion reduction.
- (10) Watzky, M. A.; Finke, R. G. *Chem. Mater.* **1997**, *9*, 3083.
- (11) Perez-Maqueda, L. A.; Matijevic, E. *Chem. Mater.* **1998**, *10*, 1430.
- (12) TEM images were recorded on a JEOL 1200EX microscope at 120 kV. Samples for TEM analysis were prepared by drop-casting films of the PTA nanoparticles onto carbon-coated TEM grids. Spot-profile EDX analysis of Au core–Ag shell nanoparticles was carried out on solution-cast films on Si (111) wafer in a Leica Stereoscan scanning electron microscope equipped with a Phoenix EDX attachment.

JA034972T